



Phase formation sequence, magnetic and structural development during solid-state reactions in 72Pt/28fcc-Co (001) thin films

V.G. Myagkov ^{a,*}, L.E. Bykova ^a, V.S. Zhigalov ^a, A.A. Matsynin ^a, D.A. Velikanov ^a, G.N. Bondarenko ^b

^a Kirensky Institute of Physics, Russian Academy of Sciences, Siberian Branch, Krasnoyarsk, 660036, Russia

^b Institute of Chemistry and Chemical Technology, Russian Academy of Sciences, Siberian Branch, Krasnoyarsk, 660049, Russia



ARTICLE INFO

Article history:

Received 13 August 2016

Received in revised form

10 February 2017

Accepted 24 February 2017

Available online 24 February 2017

Keywords:

L1₀ CoPt

L1₂ CoPt₃

Solid state reactions

Phase formation sequence

Perpendicular magnetic anisotropy

Magnetic rotatable anisotropy

ABSTRACT

The phase formation sequence during the thermally induced solid-state reaction between polycrystalline Pt and epitaxial fcc-Co (001) films in the Pt/fcc-Co(001) bilayers are systematically examined using X-ray diffraction and magnetic measurements. The films have nominal atomic ratio Co:Pt = 28:72 and total thickness 300–400 nm. Annealing to the temperature of 375 °C does not change the structural and magnetic properties of the films; this is indicative of the absence of considerable mixing at the Co/Pt interface. With the subsequent increase of the annealing temperature, the phase formation in the Pt/fcc-Co(001) bilayers has been found to have two temperature (375 °C–575 °C and 575 °C–825 °C) intervals. Solid-state reaction between Pt and Co starts above 375 °C, and nanoclusters containing the ordered L1₀ phase epitaxially intergrow with the disordered A1 phase of the composition CoPt₃ form and exist in the first temperature interval. The distinctive feature of the first interval is the formation of in-plane rotatable magnetic anisotropy. In the second temperature interval, the (L1₀ + A1) two-phase mixture grows into the ordered L1₂-CoPt₃ phase leading to the disappearance of rotatable anisotropy. Possible origin of the rotatable magnetic anisotropy is discussed. The first magnetocrystalline anisotropy constant of L1₂-CoPt₃ has the maximum value of $-5.0 \cdot 10^5$ egr/cm³ and order parameter 0.55 at 675 °C. A careful analysis of thin film solid-state reactions implies the existence of low-temperature transformation (~375 °C) on the Pt-rich side of the Co-Pt system.

© 2017 Elsevier B.V. All rights reserved.

1. Introduction

The Pt-rich Co_{1-x}Pt_x ($x > 0.7$), including CoPt₃ alloy films, has attracted a great deal of attention because of strong perpendicular magnetic anisotropy (PMA), which is important for a large number of practical applications. However, the origin of PMA in these films is not properly understood because it is not expected either in disordered A1- CoPt₃ or ordered L1₂-CoPt₃ phases. Basic models developed to explain the PMA in these films are analogous to the multilayer case and are attributed to the formation of preferentially oriented to the film plane of the two-dimensional fcc Co nanoclusters within the Pt-rich matrix [1–10].

It is generally known that PMA is uniaxial anisotropy. Recently, high rotatable magnetic anisotropy (RMA), overcoming the demagnetization anisotropy energy, was obtained in epitaxial

L1₀CoPt(111) films after the solid-state reaction in Co/Pt(111) bilayers [11]. The key feature of RMA is the rotation of the easy anisotropy axis behind the rotating magnetic field. In L1₀CoPt(111) samples in magnetic fields above the coercive force, the easy axis can be oriented in any spatial (in-plane and out-of-plane) direction. It was concluded that the high RMA can be one of PMA sources in Co_xPt_{1-x} films [11]. Despite a large number of papers explaining the origin of the PMA in Co_xPt_{1-x} thin films [1–10], RMA in Co_xPt_{1-x} thin films is described in two experimental studies only. Park et al. reported Co_{0.47}Pt_{0.53} alloy films in which the location of the easy axis is not clear for the samples annealed above 500 °C [7]. Unfortunately, this fact is not interpreted correctly as the out-plane RMA phenomena. The small in-plane RMA was also observed in Co_xPt_{1-x} (Pt ~ 25 at%) films [12]. Magnetic characteristics of these films strongly depend upon fabrication methods and thermal treatment and other parameters, including the nature of the substrate, deposition temperature and annealing temperatures. The conventional methods of Co_xPt_{1-x} film preparation on a substrate at

* Corresponding author.

E-mail address: miagkov@iph.krasn.ru (V.G. Myagkov).

various growth temperatures reported in the literature are sequential sputtering deposition and electron beam co-evaporation from Co and Pt sources. A large number of studies have addressed the phase formation between elemental Pt and Co layers in bilayers and multilayers [13–25]. However, the conditions of the phase formation at the Co/Pt interface currently remain poorly analyzed.

In this work, we describe the solid-state reaction between polycrystalline Pt with polycrystalline Co and epitaxial fcc-Co(001) films. The final goal is to reveal a significant correlation between phase formation sequence and structural and magnetic transformations forming in the 72Pt/28fcc-Co bilayers after thermal annealing up to 825 °C. In addition, in numerous studies the origin of the PMA and the contribution of RMA to PMA remain unnoticed.

2. Experiment

The epitaxial Pt/fcc-Co(001) bilayers and polycrystalline Pt/Co bilayers were prepared by subsequent deposition of Co and Pt films on a freshly cleaved (001) surface of the MgO and glass substrate. Previously, the substrates were degassed at 350 °C for 1 h. The Co layer on the MgO(001) substrate was deposited at the pressure of 10^{-6} Torr and the temperature of 250 °C; this oriented the growth of fcc-Co(001) layer on MgO(001) with epitaxial relationship fcc-Co(001)[100] || MgO(001)[100] [26]. The fcc-Co(001)/MgO(001) films had a fourfold magnetic anisotropy with the constant K_1 coinciding with the first magnetocrystalline anisotropy constant of cubic cobalt fcc-Co ($K_1^{\text{fcc}-\text{Co}} = -(5.5-6.5) \cdot 10^5$ erg/cm³) [26]. The $K_1^{\text{fcc}-\text{Co}}$ is negative because the easy magnetization axes of the fcc-Co(001) film coincided with the [110] and [1–10] directions, which are the projections {111} on the (001) plane of the MgO substrate. The top Pt layer was deposited at room temperature to prevent reaction between Co and Pt during the deposition. The thickness of the reacting Co and Pt layers, determined by the X-ray spectral fluorescent method, was ~80 and ~320 nm, respectively. This thickness ratio is close to the stoichiometry for CoPt₃. The mean chemical composition determined by EDS microanalysis was Co₂₈Pt₇₂. X-ray pattern did not contain Pt reflections; this means that the nanocrystalline Pt layer grows on the fcc-Co(001) (Fig. 1a). However, polycrystalline Pt layer grown on the polycrystalline Co film contained (111), (200), (220) peaks (Fig. 5a). The most plausible hypothesis of the essentially different Pt growth is that heat conductivity of MgO is about two orders of magnitude higher than of the glass. Therefore, deposited Pt atoms on Co/MgO are subject to a high undercooling rate, which is considerably higher than on Co/glass substrate. As a result the nanocrystalline and polycrystalline structures are formed on MgO and glass substrates, respectively. As is known, nanocrystalline structures are frequently observed in metallic glasses under a deep undercooling. The deposition of the Pt layer did not change magnetic properties of the fcc-Co(001) and Co films. These data provide clear evidence that the initial samples are Pt/fcc-Co(001) and Pt/Co polycrystalline bilayers.

Initial Pt/fcc-Co(001) samples were annealed for 1 h from 25 °C to 825 °C with a step of 50 °C. The formed phases were identified with DRON-4-07 diffractometer (CuK α radiation). The epitaxial relationships between MgO(001), reacting Pt, Co films, and the Co_xPt_{1-x} layer formed in the reaction products were X-ray studied with PANalytical X'Pert PRO diffractometer with a PIXcel detector. The CuK α radiation monochromatized by a secondary graphite monochromator was used in the instrument. The saturation magnetization M_s and the coercivity H_c were measured with a vibration magnetometer in magnetic fields up to 22 kOe. Torque curves were measured on a torque magnetometer with a sensitivity of $3.76 \cdot 10^{-9}$ Nm and a maximum magnetic field of 10 kOe. All measurements were performed at room temperature.

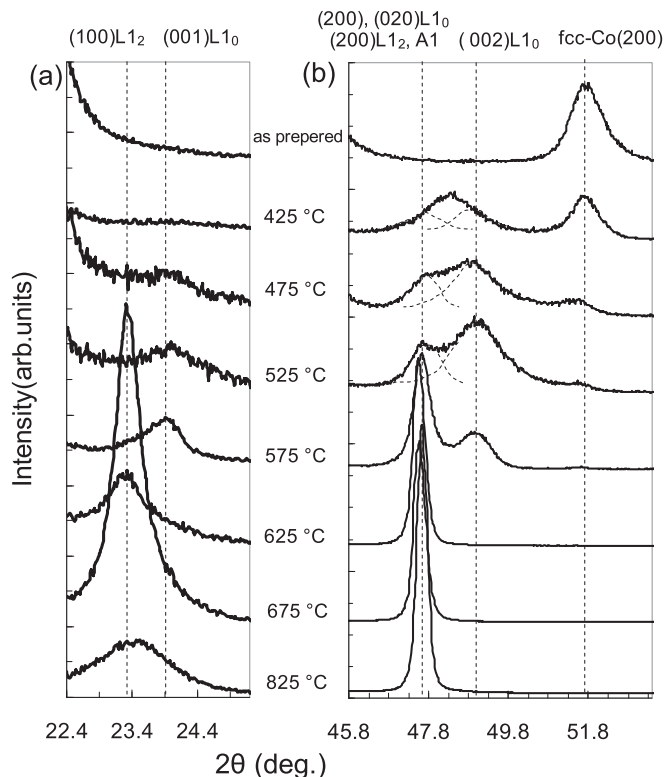


Fig. 1. Symmetrical X-ray scans through the (001)L₁₀ and (001)L₁₂ (a), the (002)L₁₀, (200)+(020)L₁₀, (200)A₁, (002)L₁₂ and (002)Co (b), reflections of epitaxial 72Pt/28Co(001) thin film before and after annealing (c). The annealing temperature changed from 375 °C to 825 °C.

3. Results

3.1. Phase transformations in 72Pt/28Co(001) thin films at increasing annealing temperature

3.1.1. X-ray studies

Fig. 1 shows XRD profiles of the as-deposited film and after annealing at temperatures from 375 °C to 825 °C for 1 h. Up to ~375 °C, the X-ray patterns of the Pt/fcc-Co(001) bilayers did not change; this is indicative of the absence of mixing and reaction between the Pt and Co layers. Analysis of diffraction data shows two (375 °C – 625 °C and 625 °C – 825 °C) temperature intervals. In the first temperature intervals after annealing at 375 °C, strong (200) fcc-Co peak began decreasing and weak (001) and {200} reflections from the ordered L₁₀ and disordered A₁ phases appeared. The (001) reflection with an interplanar spacing $d_1 = 0.372$ nm appears at approximately 24° and it is an essential sign of the L₁₀ phase only. It is important to note that the nonequilibrium process of mixing Co and Pt layers above 375 °C immediately results in the ordered L₁₀ phase. Above 425 °C X-ray diffraction reflections appear with interplanar spacings $d_2 = 0.191$ nm and $d_3 = 0.186$ nm. We associate d_1 and d_3 peaks with the (001) and (002) reflections from the Z-variant of ordered L₁₀ phase. The d_2 peak may belong to the (200) and (020) reflections from the in-plane X-, Y- variants of L₁₀, respectively, and (200) of disordered A₁ (Fig. 1b). These peaks progressively increase with annealing temperatures up to 575 °C, as a result of increasing volume fractions of L₁₀ and A₁ phases. After annealing at 575 °C intensity ratio $I(200)/I(002) \sim 3.2$, it is appreciably more than 2, which corresponds to the complete ordered L₁₀ with equal the volume fractions of X-, Y-, Z- variants. This suggests that besides L₁₀ a considerable proportion of the disordered A₁ was

formed in the first (375 °C – 575 °C) temperature interval. Total disappearance of the (001)L₁₀ and (002)L₁₀ peaks above 625 °C clearly shows the existence of the L₁₀ phase only in (375 °C – 625 °C) temperature region (Fig. 1a). Chemical composition of 72Pt/28Co film, an interplanar spacing $d_2 = 0.191$ nm value and the absence of superstructure reflection are evidence that A1 has CoPt₃ stoichiometry. Although the bulk phase diagram for the Co-Pt alloy system in Pt-rich part at low temperatures shows L₁₀ and L₁₂, we observed in 72Pt/28fcc-Co(001) films in the (375 °C – 575 °C) temperature interval only L₁₀ and A₁ phases. In the literature review for Pt-rich Co_xPt_{1-x} films, it has been reported that no superstructure spots come from L₁₂ ordering for deposited CoPt₃ on NaCl(001) even at 670 K [27]. A.L. Shapiro et al. showed that L₁₂ long-range chemical order is present in epitaxial (100), (110), (111) and polycrystalline Co_{0.25}Pt_{0.75} and Co_{0.35}Pt_{0.65} films only at 550 °C–700 °C [28], which is close to the second (575 °C–825 °C) temperature interval of our work.

The diffraction pattern radically changes after annealing at temperatures above 625 °C. The (001)L₁₀ peak vanishes completely, while the (100)L₁₂ and (200)L₁₂ peaks progressively increase up to 675 °C (Fig. 1). This suggests that the ordered L₁₂-CoPt₃ phase prevails above 625 °C and its structural perfection and order parameters grow up to 675 °C. In-plane epitaxial relationship between L₁₂-CoPt₃ film and substrate MgO(001): (100)[011]CoPt₃ || (100)[011]MgO was found by asymmetrical X-ray diffraction. This relationship inherits all fcc Co-Pt alloy films on MgO(001) substrate [13,29,30]. However, the above order-disorder transition temperature (685 °C) of the L₁₂-CoPt₃ only partially transforms to the A₁ phase, and it is steady up to 825 °C. In summary, the epitaxial mixture of the ordered L₁₀ and disordered A₁ of the CoPt₃ composition simultaneously start at Pt/Co interface above 375 °C and grows into the ordered L₁₂-CoPt₃ above 675 °C.

3.1.2. In-plane magnetic torque studies and magnetic characterization

The above X-ray diffraction results have been correlated with the in-plane torque curve modifications of 72 Pt/28fcc-Co(001) thin film at increasing annealing temperature. The torque measurements show easy in-plane magnetization axis for all annealing temperatures. Fig. 2 shows a series of in-plane torque curves L(ϕ) of 72Pt/28fcc-Co(001) bilayer at different annealing temperatures. As-prepared samples 72Pt/28fcc-Co(001) possessed the fourfold anisotropy constant $K_4 = -2.1 \cdot 10^5$ erg/cm³, defined by the first magnetocrystalline anisotropy constant of epitaxial fcc-Co(001) layer ($K_1 = -6 \cdot 10^5$ erg/cm³) [26]. The K_4 constant did not change up to 375 °C and this is confirmed by the absence of structural transformations in the fcc-Co(001) layer. In the first temperature interval (375 °C – 625 °C) after annealing at 425 °C, the torque curves show rotatable magnetic anisotropy (RMA) [11] with L^{rot} constant, reaching its maximum when annealed at 575 °C (Figs. 2 and 3). At the big values of magnetic field rotation angle ϕ , the torque curves L(ϕ) consist of fourfold component $\frac{1}{2}K_4 \sin 4\phi$ and ϕ -independent + L^{rot} and - L^{rot} components for clockwise and counterclockwise rotations, respectively (1).

$$L(\phi) = \pm L^{\text{rot}} + \frac{1}{2}K_4 \sin 4\phi \quad (1)$$

The RMA formation confirms the X-ray studies indicative of the beginning of mixing of the Pt and Co layers and the synthesis two-phase (L₁₀ + A₁) mixture above 375 °C. In the second temperature interval (575 °C – 825 °C) after annealing at 625 °C, the L^{rot} constant sharply decreases and drops at 675 °C. At the same time the K_4 constant reaches its maximum at 675 °C and insignificantly decreases after annealing above 675 °C (Fig. 3). The existence of the RMA and (L₁₀ + A₁) mixture in the first temperature interval and

the disappearance of L₁₀ in the second temperature interval is direct evidence that the RMA origin is a characteristic feature of epitaxially intergrown of the L₁₀ and A₁ phases.

The dependence of the L^{rot} constant, the fourfold anisotropy constant K_4 , and saturation magnetization M_S as a function of annealing temperature are summarized in Fig. 3. Fig. 3a shows that L^{rot} reaches its peak value at 575 °C and the RMA phenomenon exists only in the first temperature interval. K_4 in the first temperature interval is the fourfold magnetic anisotropy constant of the (L₁₀ + A₁) mixture independent of the annealing temperature up to 575 °C. K_4 sharply increases above 625 °C because it is associated with (L₁₀ + A₁) → L₁₂-CoPt₃ transformation; therefore, it is equal to first magnetocrystalline constant $K_1^{\text{L12-CoPt3}}$ of L₁₂-CoPt₃.

Fig. 3b shows that within the limits of experimental error the saturation magnetization of Pt/fcc-Co(001) films does not change during the annealing process, i.e. contributing to magnetization of all phases of the phase sequence are Co atoms only. In-plane and out-of-plane M-H loops are shown in Fig. 4 for samples (L₁₀ + A₁) annealed at 575 °C and for L₁₂-CoPt₃ annealed at 675 °C. In both cases all samples exhibit the in-plane easy axis, same magnetization $M_S = 390$ emu/cc and not high coercivity.

3.2. Phase transformations in polycrystalline 72Pt/28Co thin films at increasing annealing temperature

The evidence of formation of the two-phase mixture of disordered A₁ of the CoPt₃ composition and ordered L₁₀ phases, which possess RMA, was also confirmed by the investigation of solid-state reactions in polycrystalline 72Pt/28Co thin films.

3.2.1. X-ray studies

The as-prepared 72Pt/28Co sample exhibits only Pt and Co peaks, indicating a formation bilayer structure in the film (Fig. 5a). Fig. 5b,c shows the XRD profiles of the 72Pt/28Co sample after annealing at 425 °C and 525 °C. In both cases, synthesized samples show (111), (200) CoPt₃ and (001), (200), (002) CoPt peaks. These results along with the existence of the superstructure (001)L₁₀ and the absence of (001)L₁₂ peaks uniquely indicate that the L₁₀ and A₁ composition CoPt₃ phases simultaneously form at the Pt/Co interface and, as a result, the chemically intergrown L₁₀ and A₁ nanocrystallites prevail in the reaction product in the first temperature interval (375 °C – 575 °C).

3.2.2. In-plane magnetic torque studies

As-prepared polycrystalline samples 72Pt/28Co have insignificant in-plane uniaxial anisotropy. Fig. 6 shows the in-plane torque curves L(ϕ) at annealing temperatures 425 °C and 525 °C. After annealing above 425 °C, minor in-plane RMA formed and L^{rot} constant grows with annealing temperature up to 525 °C. The torque curves L(ϕ) are given over the range of $0 \leq \phi \leq 720^\circ$ to show that, in contrast to the classic magnetic anisotropies, the torque curves of RMA cannot be described by sinusoidal dependence. It is important to note that within the limits of the experimental accuracy the values L^{rot} coincide for polycrystalline Pt/Co and Pt/fcc-Co(001) bilayers. Hence, it follows that the origin of RMA is not associated with film-substrate stress or fcc-Co(001) epitaxial growth.

4. Discussion

Thin-film solid state reactions are known to be specified by the initiation temperature T_{in} and the first phase arising at the film interface when the temperature of sample T_S exceeds T_{in} ($T_S > T_{\text{in}}$). At increasing annealing temperatures, other phases may occur and

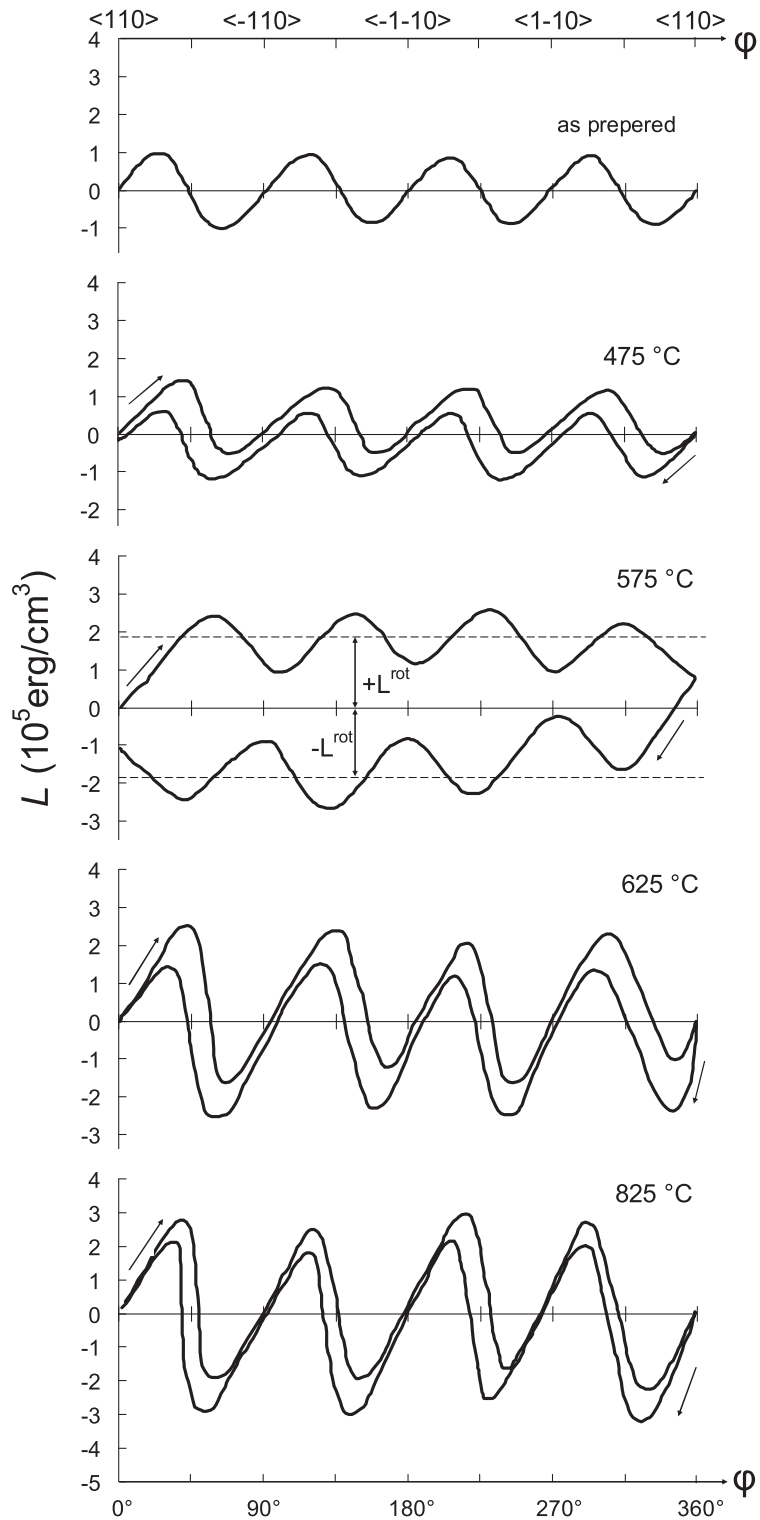


Fig. 2. Evolution of in-plane torque curves of epitaxial 72Pt/28Co(001) thin film. Measurements were made at 1.0 T at room temperature. The hysteresis between clockwise and counterclockwise rotations starts at 425 °C, reaches the maximum value at 575 °C and is minor after annealing above 625 °C.

form the phase sequence [31–34]. In most thin film solid state reactions, the initiation temperatures T_{in} have low value ($T_{in} < 500$ °C). However, some reactions occur around room [35,36] or even at cryogenic [37–40] temperatures. Therefore, to explain the atomic transport through the reaction product layer we should assume that the diffusivity in the reaction state exceeds the

diffusivity in the solid state by a factor of more than 10^{11} [41–43]. Although the threshold of the reaction (initiation temperature T_{in}) was discovered in the first studies of the thin-film solid state reactions, in modern research it is not taken into account, because it does not match with the diffusion mechanism. In diffusion studies, it was assumed that the initiation temperature of a reaction T_{in} is a

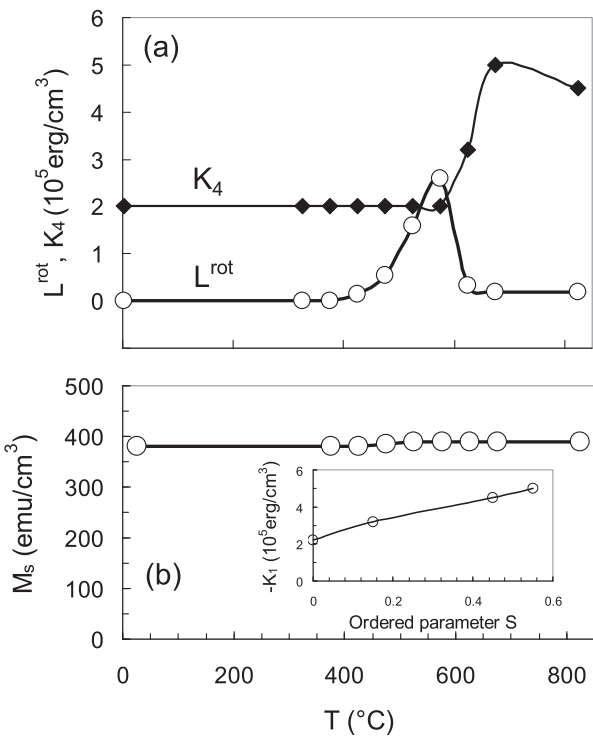


Fig. 3. Variations of rotatable magnetic anisotropy constant L_{rot} and the fourfold anisotropy constant K_4 (a) and saturation magnetization M_s (b) as a function of annealing temperature. Inset shows the first magnetocrystalline anisotropy constant K_1 of the $\text{L}_{12}\text{-CoPt}_3$ phase as a function of chemical ordering parameter S .

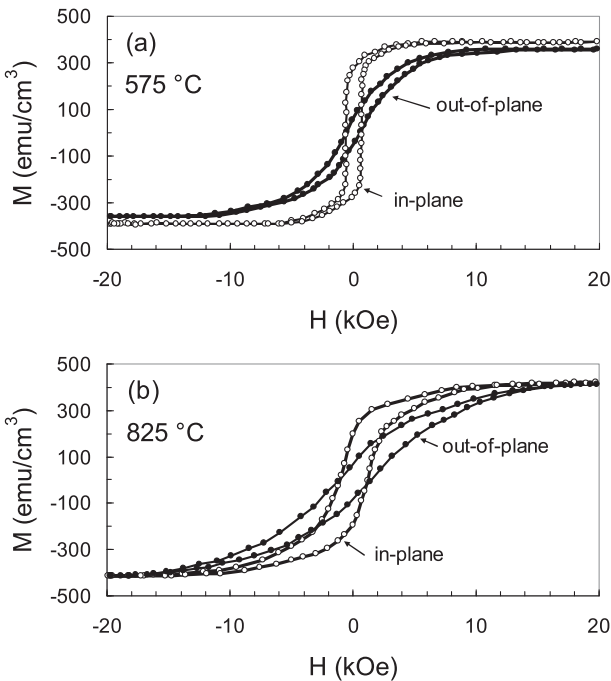


Fig. 4. In-plane and out-of-plane M-H loops of L_{10} + A_{11} two-phase mixture at 575 °C (a) and $\text{L}_{12}\text{-CoPt}_3$ at 675 °C (b).

kinetic quantity that depends on the heating rate. However, there is an objection against this assumption. As the temperature is increased, the reaction rate increases slower than the rate of heating of the reaction mixture. This leads to an experimental shift

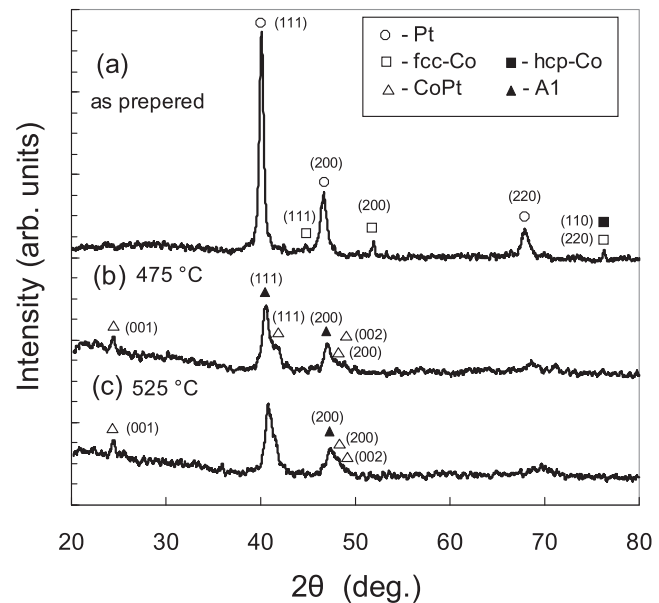


Fig. 5. Symmetrical X-ray scans of polycrystalline 72Pt/28 thin film before (a) and after annealing at 475 °C (b), 525 °C (c).

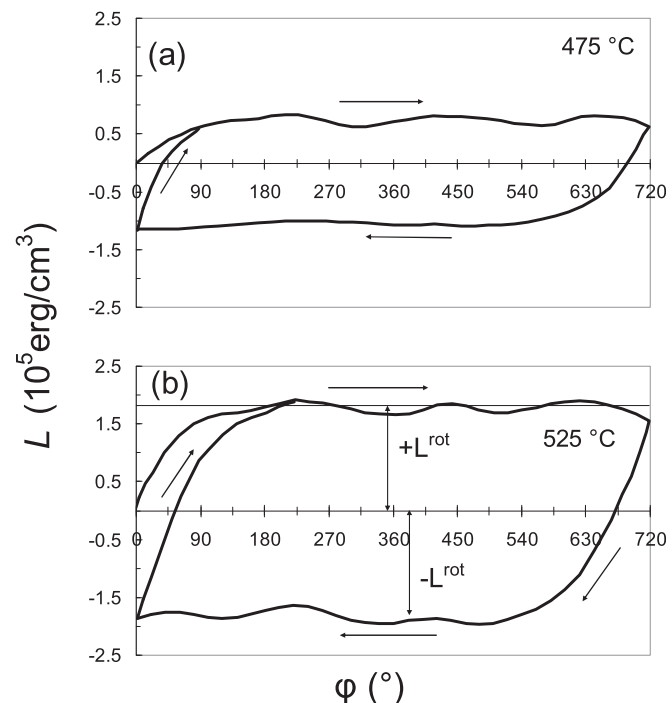
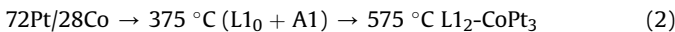


Fig. 6. The evolution of in-plane torque curves of polycrystalline 72Pt/28Co thin film after annealing at 475 °C (a), 525 °C (b).

of initiation temperature T_{in} into high temperatures. In fact, below T_{in} the atomic mixing at the interface is minor and the first phase did not identify. Above T_{in} the observed atomic mixing starts simultaneously with the first phase formation and the reaction rate strongly accelerates with the increase ($T-T_{\text{in}}$). Based on an analysis of low-temperature thin films reaction and the μm -range atomic transfer of the reacting atoms, we concluded that the diffusion plays a nonprincipal role, while the chemical interactions control the atomic transfer, structural rearrangements and synthesis phases in the solid state [41–43].

Within the experimental accuracy initiation temperatures, T_{in} in many bilayer films has been shown to coincide with the temperatures of solid-state structural transformations T_K ($T_{in} = T_K$). The equality $T_{in} = T_K$ is valid for order-disorder phase transitions in Au–Cu ($T_{in} = T_K = 240$ °C) [44,45] and Fe–Pd (450 °C) [42,46]; for eutectoid decompositions in Fe–Ni (350 °C) [43,47,48] and Fe–Cu (850 °C) [49]; for martensitic transformations in Al–Ni (180 °C) [50], Ti–Ni (~100 °C) [51], and Au–Cd (60 °C) [52,53] and for other phase transformations [54–56]. It is interesting to note that intensive studies of the nature of ferromagnetism in diluted $Mn_{1-x}Ge_x$ ($x > 0.95$) solid solutions revealed low-temperature ($T_K \sim 120$ °C) spinodal decomposition in the Mn–Ge system [57–59]. Recently, we showed that the solid-phase reaction in Mn/Ge films begins at the temperature of spinodal decomposition $T_{in} = T_K \sim 120$ °C [41,60,61]. Consequently, solid-state reactions in thin films occur only in binary systems having solid-state structural transformations and the same chemical interactions control the solid-state reactions in thin films and respective solid-state transformations. The equality $T_{in} = T_K$ assumes that if the initiation temperature T_{in} is known, it supposes the possible existence of structural transformation at temperature T_K in a given binary system.

The studies presented in this article and in Ref. [11] definitively show that above initiation temperature $T_{in}^1 \sim 375$ °C, the ($L_{10} + A_1$) two-phase mixture forms in the 72Pt/28Co bilayer and, above the initiation temperature $T_{in}^2 \sim 575$ °C, it grows into the ordered $L_{12}-CoPt_3$. It corresponds to the phase formation sequence (2).



On the basis of the above-mentioned facts, we propose the existence of two solid-state transformations in the Pt-rich concentration region of the Co-Pt system.

- (i) The first transformation, which occurs above 375 °C, is associated with the phase decomposition of solid solution CoPt into a two-phase mixture. Chemically disordered solid solution in the Co_xPt_{1-x} thin films may form by quenching from high to room temperature or in the films grown below 375 °C [1–10]. In both cases after annealing above 375 °C the ($L_{10} + A_1$) compound has to form. Earlier papers suggested that the source of perpendicular magnetic anisotropy in Co_xPt_{1-x} films was associated with the phase-separated Pt-rich and Co-rich regions or Co clustering in $CoPt_3$ films growing above 400 °C [1–10]. Rooney et al. postulate that this phase separation occurs via spinodal decomposition [6]. Our results confirm the existence of phase separation in the Pt-rich side of the Co–Pt system above 375 °C. This considered, we believe that chemical interactions between Co and Pt start above ~375 °C and are the driving force for the solid-state reaction (1) and phase decomposition of Co_xPt_{1-x} thin films into the mixture of L_{10} (Co-rich regions) and A_1-CoPt_3 (Pt-rich regions).
- (ii) The second ($L_{10} + A_1$) → $L_{12}-CoPt_3$ transformation starts at $T_{in} \sim 575$ °C. On the basis of the above results; we suggest that this temperature is equal with the order-disorder phase transition temperature in 72Pt28Co alloys ($T_{in} = T_K \sim 575$ °C). However, it does not coincide with 685 °C, the order-disorder temperature of the bulk $Co_{28}Pt_{72}$ samples. Though Monte Carlo simulations predict the $L_{12} \rightarrow A_1$ transition at 850 K (577 °C) for the $CoPt_3$ alloys [62], it is reasonable to suggest that a concentration in homogeneities, structural defects and intergrain stresses are main factors that decrease the order-disorder temperature in thin films and modify the bulk Co–Pt equilibrium phase diagram.

Phase transformations and magnetic properties in epitaxial Pt/fcc-Co(001) and Co/Pt(111) films have been observed to be correlated with an increase of annealing temperature up to 825 °C. In our previous work [11] we demonstrated that, in the epitaxial film systems Co/Pt(111) of equiatomic composition, the magnetically hard $L_{10}CoPt(111)$ phase epitaxially intergrows with the disordered $CoPt_3$ phase. In both cases ($L_{10} + A_1$) two-phase mixing occurs above 400 °C. However, RMA constant for Co/Pt(111) ($L_{rot} = 2.2 \cdot 10^6$ erg/cm³) films is more than tenfold in the Pt/Co(001) ($L_{rot} = 2.2 \cdot 10^5$ erg/cm³) samples. It is notable that the L_{10} phase and RMA simultaneously disappears above 575 °C. This suggests that the RMA origin is specified by the L_{10}/A_1 interface stresses, which affect the resulting RMA properties. Undoubtedly, the RMA value strongly depends on the composition, crystallography and structural features of the ($L_{10} + A_1$) compounds, which play the key role in the RMA formation. The exchange interaction between the antiferromagnetic and ferromagnetic grains and magnetostriction are the most frequently used to explain RMA origin in thin films [11]. However, L_{10} and A_1 are ferromagnetic phases; therefore, our results cannot be explained by the ferro-antiferromagnetic exchange coupling model. Phase boundaries are well-known to generate the striking physical properties of the functional materials [63]. For example, the coherent phase decomposition near the morphotropic phase boundary (MPB) enhances electro-mechanical properties of the ferroelectric materials. The ferromagnetic systems around magnetic MPB separating two magnetic phases with different crystal symmetries may reveal the significant enhancement of magnetic and magnetostrictive properties [64–66]. Although RMA origin still remains unknown, among possible explanations is the existence of epitaxial intergrown L_{10} and A_1 phases, inducing large magnetostriction and magnetic-field-induced strain, creating uniaxial anisotropy with an easy axis along the direction of the magnetic field.

Following equation (1) in the first temperature interval in addition to L^{rot} , there is a contribution of the fourfold anisotropy with constant K_4 into the magnetic anisotropy of the ($L_{10} + A_1$) sample (Fig. 2). There are no contributions from unidirectional anisotropy and uniaxial anisotropy. It is reasonable to suggest that K_4 constant is determined by magnetocrystalline anisotropy constants of L_{10} and A_1 phases.

Magnetocrystalline anisotropy energy E_K for the tetragonal L_{10} crystal per unit volume of the sample (V) has form (3) [67].

$$E_K = E_0 + K_1 \sin^2 \phi + K_2 \sin^4 \phi + K_3 \cos^2 \alpha \cdot \cos^2 \beta \quad (3)$$

where ϕ is the angle between magnetization M_S and [001] c axis and α and β are the angles between magnetization M_S and the [100] and [010] axes, respectively. The first anisotropy constant $K_1^{L_{10}} = 4.8 \cdot 10^7$ erg/cm³ was estimated for L_{10} -CoPt bulk samples, but as of today the values of $K_2^{L_{10}}$ and $K_3^{L_{10}}$ are not known [68,69]. It is common knowledge that specific for L_{10} magnetic film materials (including L_{10} -CoPt films) is the formation of the three equivalent X-, Y-, Z- variants, which have with respect to the MgO substrate the epitaxial orientation relationships (4) [70,71].

$$\begin{aligned} & A_1 (001) [010] \parallel MgO (001) [010]; \\ & Z - L_{10} (001) [001] \parallel MgO (001) [001]; \\ & Z - L_{10} (001) [010] \parallel MgO (001) [010]; \\ & Z - L_{10} (001) [001] \parallel MgO (001) [010]. \end{aligned} \quad (4)$$

Assume the three variants of the L_{10} grains to be exchange coupled and their volume fractions to be the same $f_X = f_Y = f_Z = 1/3$, neglecting the basal plane anisotropy $K_3^{L_{10}}$ in expression (3) and taking account of relationships (4), the contribution $E_K(L_{10})$ from the L_{10} to magnetic anisotropy energy of the ($L_{10} + A_1$) films may be

found by using of expression (5).

$$E_K(L1_0) = E_0 + 2/3K_2^{L10} (\beta_1^2\beta_2^2 + \beta_2^2\beta_3^2 + \beta_1^2\beta_3^2) \quad (5)$$

where β_i ($i = 1, 2, 3$) are the direction cosines of the magnetization. It is surprising that first magnetocrystalline constant K_1^{L10} makes no contribution to magnetic anisotropy films with X-, Y-, Z- variants of the $L1_0$ phase. The magnetic anisotropy energy $E_K(L1_0 + A1)$ of the $(L1_0 + A1)$ films together with the contribution $2/3K_2^{L10}V_{L10}/V$ contains the contribution $K_1^{A1}V_{A1}/V$ from the disordered $A1$ phase (6).

$$E_K(L1_0 + A1) = E_0 + \{2/3K_2^{L10}V_{L10}/V + K_1^{A1}V_{A1}/V\} \times (\beta_1^2\beta_2^2 + \beta_2^2\beta_3^2 + \beta_1^2\beta_3^2) \quad (6)$$

where V_{L10}/V and V_{A1}/V are the relative volumes of the $L1_0$ and $A1$ phases, respectively. Note that the magnetic anisotropy of the exchange coupled three X-, Y-, Z- variants of the $L1_0$ and disordered $A1$ grains is described by cubic effective anisotropy constant $K_{eff}V = 2/3K_2^{L10}V_{L10} + K_1^{A1}V_{A1}$. All obtained constants have a minus sign because after annealing the easy axes do not change the [110] and [1–10] directions. An important point is that the relation between V_{L10} and V_{A1} changes with the increase of the annealing temperature, and the value $V_{L10} \sim 0$ at 575 °C, but at the same time the constant $K_4 = -2.1 \cdot 10^5$ erg/cm³ remains constant (Fig. 3a). Hence, it follows that the absolute value of the anisotropy constants $2/3K_2^{L10}$ and K_1^{A1} does not exceed 2.1×10^5 erg/cm³ because of low values of the second magnetocrystalline anisotropy constant of the $L1_0$ phase $K_2^{L10} \sim -3.1 \times 10^5$ erg/cm³ and the first magnetic anisotropy constant of disordered $A1$ phase $K_1^{A1} = -2.1 \times 10^5$ erg/cm³. The estimated value of K_1^{A1} is close to the bulk sample value of the disordered cubic $Pt_2Co_{48} \approx -6 \cdot 10^5$ erg/cm³ [69].

To summarize, it has been proved that the films consist of two-phase mixture of $L1_0$ with three variants, and disordered $A1$ are soft magnetic materials with low magnetic anisotropy constant $K_{eff} = -2.1 \cdot 10^5$ erg/cm³ and, accordingly, low coercive force $H_C \sim 700$ Oe (Fig. 4a).

As shown above, in the second temperature interval, only the ordered $L1_2$ - $CoPt_3$ phase forms; therefore, the fourfold anisotropy with constant K_4 is equal to the first magnetocrystalline anisotropy constant $K_1^{L12-CoPt3}$ of the $L1_2$ - $CoPt_3$ phase. Chemical ordering parameter S was found after annealing at 625 °C ($S = 0.05$), 675 °C ($S = 0.55$) and 825 °C ($S = 0.45$) in the ordered $L1_2$ - $CoPt_3$ films by the ratio of the measured integrated intensity of the (001) superlattice and (002) fundamental diffraction peaks taking into account the structure factors, the multiplicity factors, the Lorentz-polarization factors and ignored temperature and absorption effects. Inset to Fig. 3 shows the plot of the first magnetocrystalline anisotropy constant $K_1^{L12-CoPt3}$ of the $L1_2$ - $CoPt_3$ phase as a function of chemical ordering parameter S . Following Fig. 3 results, the maximum value $K_1^{L12-CoPt3} = -5.0 \times 10^5$ erg/cm³ matches the maximum value of the ordering parameter $S = 0.55$ at 675 °C. However, above the order-disorder temperature 685 °C the $L1_2$ - $CoPt_3$ phase transforms only partially into disorder $A1$ - $CoPt_3$ phase because at 825 °C values of $K_1^{L12-CoPt3} = -4.5 \cdot 10^5$ erg/cm³ and $S = 0.45$ are insignificantly less than at 675 °C. The probable reason for the retardation of the $L1_2 \rightarrow A1$ transformation is the epitaxial intergrowth of the $L1_2$ - $CoPt_3$ with MgO substrate. The coercive force of the $L1_2$ - $CoPt_3$ ($S = 0.55$) is $H_C \sim 1.3$ kOe (Fig. 4b) and it is close to epitaxial $CoPt_3$ (001) films $H_C \sim 2.0$ kOe grown on $MgO(001)$ substrate at 400 °C [72].

5. Conclusion

Solid-state reaction in epitaxial and polycrystalline 72Pt/28Co

on $MgO(001)$ and glass substrate, respectively, has been studied over a range of annealing temperatures from 25 °C to 825 °C. The reaction between Pt and Co starts at 375 °C and has two temperature intervals. At the first interval (375 °C – 575 °C) the ordered $L1_0$ and disordered $A1$ two-phase mixture forms, and in the second temperature interval (625 °C – 825 °C) this mixture transforms into the ordered $L1_2$ - $CoPt_3$ phase. In the first temperature interval, the discovered in-plane rotatable anisotropy is associated with the $(L1_0 + A1)$ mixture. The rotatable anisotropy disappears above 575 °C because at the second interval the $(L1_0 + A1)$ mixture grows into ordered $L1_2$ - $CoPt_3$ phase. The first magnetocrystalline anisotropy constants were estimated as $-2.1 \cdot 10^5$ erg/cm³ and $-5.0 \cdot 10^5$ erg/cm³ for disordered $A1$ and for $L1_2$ - $CoPt_3$ with order parameter 0.55, respectively. The phase formation sequence has been analyzed using the concept in which the same chemical mechanisms control both solid state reactions and phase transformations at the nanoscale.

Acknowledgements

This study was supported by the Russian Foundation for Basic Research (Grant # 15-02-00948-a, 16-03-00069-a). The XPS and TEM studies were carried out using the facilities of the Performance Service at Krasnoyarsk Scientific Center.

References

- [1] F. Liscio, M. Maret, C. Meneghini, S. Mobilio, O. Proux, D. Makarov, M. Albrecht, Structural origin of perpendicular magnetic anisotropy in epitaxial $CoPt_3$ nanostructures grown on $WSe_2(0001)$, Phys. Rev. B 81 (2010) 125417–1–125417–9.
- [2] C. Meneghini, M. Maret, V. Parasote, M.C. Cadeville, J.L. Hazemann, R. Cortes, S. Colonna, Structural origin of magnetic anisotropy in Co-Pt alloy films probed by polarized XAFS, Eur. Phys. J. B 7 (1999) 347–357.
- [3] T.A. Tyson, S.D. Conradson, R.F.C. Farrow, B.A. Jones, Observation of internal interfaces in Pt_xCo_{1-x} ($x \approx 0.7$) alloy films: a likely cause of perpendicular magnetic anisotropy, Phys. Rev. B 54 (1996) R3702–R3705.
- [4] D. Weller, H. Brändle, C. Chappert, Relationship between Kerr effect and perpendicular magnetic anisotropy in $Co_{1-x}Pt_x$ and $Co_{1-x}Pd_x$ alloys, J. Magn. Magn. Mater. 121 (1993) 461–470.
- [5] M. Charilaou, C. Bordel, P.-E. Berche, B.B. Maranville, P. Fischer, F. Hellman, Magnetic properties of ultrathin discontinuous Co/Pt multilayers: comparison with short-range ordered and isotropic $CoPt_3$ films, Phys. Rev. B 93 (2016) 224408-1–224408-10.
- [6] P.W. Rooney, A.L. Shapiro, M.Q. Tran, F. Hellman, Evidence of a surface-mediated magnetically induced miscibility gap in Co-Pt alloy thin films, Phys. Rev. Lett. 75 (1995) 1843–1846.
- [7] S.-E. Park, P.-Y. Jung, K.-B. Kim, Magnetic properties and microstructural analysis of sputter deposited and annealed Co-Pt alloys, J. Appl. Phys. 77 (1995) 2641–2647.
- [8] S. Heinrichs, W. Dieterich, P. Maass, Modeling epitaxial growth of binary alloy nanostructures on a weakly interacting substrate, Phys. Rev. B 75 (2007) 085437–1–085437–10.
- [9] A.L. Shapiro, P.W. Rooney, M.Q. Tran, F. Hellman, K.M. Ring, K.L. Kavanagh, B. Rellinghaus, D. Weller, Growth-induced magnetic anisotropy and clustering in vapor-deposited Co-Pt alloy films, Phys. Rev. B 60 (1999) 12826–12836.
- [10] O. Cross, M. Newville, B.B. Maranville, C. Bordel, F. Hellman, V.G. Harris, Evidence for nanoscale two-dimensional Co clusters in $CoPt_3$ films with perpendicular magnetic anisotropy, J. Phys. Condens. Matter 22 (2010) 146002.
- [11] V.G. Myagkov, V.S. Zhigalov, L.E. Bykova, G.N. Bondarenko, A.N. Rybakova, A.A. Matsynin, I.A. Tambasov, M.N. Volochayev, D.A. Velikanov, High magnetic rotatable anisotropy in epitaxial $L1_0$ - $CoPt(111)$ thin films, JETP Lett. 6 (2015) 355–360.
- [12] A.N. Sorokin, A.V. Svalov, Magnetic and galvanomagnetic properties of $CoPt$ films, J. Magn. Magn. Mater. 146 (1995) 214–216.
- [13] B.M. Lairson, M.R. Visokay, E.E. Marinero, R. Sinclair, B.M. Clemens, Epitaxial tetragonal $PtCo$ (001) thin films with perpendicular magnetic anisotropy, J. Appl. Phys. 74 (1993) 1922–1928.
- [14] D.M. Artymowicz, B.M. Lairson, B.M. Clemens, Formation of ordered tetragonal $PtCo$ from epitaxial $PtCo$ multilayers, J. Cryst. Growth 169 (1996) 83–88.
- [15] J.S. Tsay, C.S. Shern, Diffusion and alloy formation of Co ultrathin films on $Pt(111)$, J. Appl. Phys. 80 (1996) 3777–3777.
- [16] C.S. Shern, C.W. Su, Y.E. Wu, T.Y. Fu, Alloying of Co ultrathin films on $Pt(111)$ with Ag buffer layers, J. Appl. Phys. 88 (2000) 705–709.
- [17] A. Markou, I. Panagiotopoulos, T. Bakas, Effects of layering and magnetic

- annealing on the texture of CoPt films, *J. Magn. Magn. Mater.* 322 (2010) L61–L63.
- [18] K. Sato, K. Yanajima, T.J. Konno, Structure and compositional evolution in epitaxial Co/Pt core–shell nanoparticles on annealing, *Thin Solid Films* 520 (2012) 3544–3552.
- [19] T.Y. Lee, D.S. Son, S.H. Lim, S.-R. Lee, High post-annealing stability in [Pt/Co] multilayers, *J. Appl. Phys.* 113 (2013), 216102–1–216102–3.
- [20] T. Das, P.D. Kulkarni, S.C. Purandare, H.C. Barshilia, Anomalous enhancement in interfacial perpendicularly magnetic anisotropy through uphill diffusion, *Sci. Rep.* 4 (2014), <http://dx.doi.org/10.1038/srep05328>.
- [21] T.Y. Lee, Y.C. Won, D.S. Son, S.H. Lim, S.-R. Lee, Effects of Co layer thickness and annealing temperature on the magnetic properties of inverted [Pt/Co] multilayers, *J. Appl. Phys.* 114 (2013), 173909–1–173909–6.
- [22] S. Bandiera, R.C. Sousa, B. Rodmacq, B. Dieny, Enhancement of perpendicular magnetic anisotropy through reduction of Co-Pt interdiffusion in (Co/Pt) multilayers, *Appl. Phys. Lett.* 100 (2012), 142410–1–142410–4.
- [23] S.-L. Jiang, X.-J. Li, Y.-W. Liu, X. Chen, Q.-Q. Liu, G. Han, G. Yang, D.-W. Wang, J.-Y. Zhang, J. Teng, G.-H. Yu, Thermally stable anomalous Hall behavior in perpendicular Co/Pt multilayers sandwiched by HfO₂ layers, *Appl. Surf. Sci.* 360 (2016) 758–761.
- [24] A. Markou, I. Panagiotopoulos, T. Bakas, Effects of layering and magnetic annealing on the texture of CoPt films, *J. Magn. Magn. Mater.* 322 (2010) L61–L63.
- [25] N. Sehdev, R. Medwal, D.C. Agrawal, S. Annapoorni, Correlation of interlayer diffusion with the stoichiometric composition of RF sputtered Pt/Co/Pt sandwiched structures, *J. Mater. Sci.* 48 (2013) 3192–3197.
- [26] V.G. Myagkov, L.E. Bykova, V.S. Zhigalov, I.A. Tambasov, G.N. Bondarenko, A.A. Matsynin, A.N. Rybakova, Solid-State synthesis, structural and magnetic properties of CoPd films, *Phys. Solid State* 57 (2015) 1018–1026.
- [27] F. Liscio, M. Maret, C. Meneghini, S. Mobilio, O. Proux, D. Makarov, M. Albrecht, Structural origin of perpendicular magnetic anisotropy in epitaxial CoPt₃ nanostructures grown on WSe₂(0001), *Phys. Rev. B* 81 (2010), 125417–1–125417–9.
- [28] A.L. Shapiro, P.W. Rooney, M.Q. Tran, F. Hellman, K.M. Ring, K.L. Kavanagh, B. Rellinghaus, D. Weller, Growth-induced magnetic anisotropy and clustering in vapor-deposited Co-Pt alloy films, *Phys. Rev. B* 60 (1999) 12826–12836.
- [29] O. Ersen, V. Parasote, V. Pierron-Bohnes, M.C. Cadiveau, C. Ulhaq-Bouillet, Growth conditions to optimize chemical order and magnetic properties in molecular-beam-epitaxy-grown CoPt/MgO(001) thin films, *J. Appl. Phys.* 93 (2003) 2987.
- [30] M. Ohtake, S. Ouchi, F. Kirino, M. Futamoto, L₁₀ ordered phase formation in FePt, FePd, CoPt, and CoPd alloy thin films epitaxially grown on MgO(001) single-crystal substrates, *J. Appl. Phys.* 111 (2012) 07A708.
- [31] J.M. Poate, K.N. Tu, J.W. Mayer (Eds.), *Thin Films-interdiffusion and Reaction*, Wiley-Interscience, New York, 1978.
- [32] E.G. Colgan, *Mater. Sci. Rep.* 5 (1990) 1–44.
- [33] R. Pretorius, C.C. Theron, A. Vantomme, J.W. Mayer, *Crit. Rev. Solid. State Mater. Sci.* 24 (1999) 1–62.
- [34] T. Laurila, J. Molarius, *Crit. Rev. Solid. State Mater. Sci.* 28 (2003) 185–230.
- [35] V. Simic, Z. Marinkovic, *J. Mater. Sci.* 33 (1998) 561–624.
- [36] A.R. Chourasia, Investigation of chemical reactivity at the M/CuO interfaces (where M = Fe, Co, or Ni), *J. Appl. Phys.* 112 (2012), 024323–1–024323–5.
- [37] M. Seyffert, A. Siber, P. Ziemann, Multiple low-temperature interface reactions: an alternative route into the amorphous state of metallic alloys, *Phys. Rev. Lett.* 67 (1991) 3792–3795.
- [38] H.-G. Boyen, G. Indlekofer, G. Gantner, H. Stupp, A. Cossy-Favre, P. Oelhafen, Intermixing at Au-In interfaces as studied by photoelectron spectroscopy, *Phys. Rev. B* 51 (1995) 17096–17099.
- [39] Th. Koch, A. Siber, J. Marien, P. Ziemann, Intermixing at Au-In and Pd-In interfaces at 90 K as observed by *in situ* Auger-electron and electron-energy-loss spectroscopy, *Phys. Rev. B* 49 (1994) 1996–2000.
- [40] A. Siber, D. Massinger, Th. Koch, P. Ziemann, Multilayers—a way to prepare metastable phases by multiple interface reactions, *Thin Solid Films* 275 (1996) 73–77.
- [41] V.G. Myagkov, L.E. Bykova, A.A. Matsynin, M.N. Volochaev, V.S. Zhigalov, I.A. Tambasov, Yu.L. Mikhlin, D.A. Velikanov, G.N. Bondarenko, Solid state synthesis of Mn₅Ge₃ in Ge/Ag/Mn trilayers: structural and magnetic studies, *J. Solid State Chem.* 246 (2017) 379–387.
- [42] V. Myagkov, O. Bayukov, Y. Mikhlin, V. Zhigalov, L. Bykova, G. Bondarenko, Long-range chemical interactions in solid-state reactions: effect of an inert Ag interlayer on the formation of L₁₀-FePd in epitaxial Pd(001)/Ag(001)/Fe(001) and Fe(001)/Ag(001)/Pd(001) trilayers, *Philos. Mag.* 94 (2014) 2595–2622.
- [43] V.G. Myagkov, V.C. Zhigalov, L.E. Bykova, G.N. Bondarenko, Long-range chemical interaction in solid-state synthesis: chemical interaction between Ni and Fe in epitaxial Ni(001)/Ag(001)/Fe(001) trilayers, *Int. J. SHS* 18 (2) (2009) 117–124.
- [44] V.G. Myagkov, L.E. Bykova, V.S. Zhigalov, A.I. Pol'skii, F.V. Myagkov, Solid-phase reactions, self-propagating high-temperature synthesis, and order-disorder phase transition in thin films, *JETP Lett.* 71 (2000) 183–186.
- [45] V.G. Myagkov, Yu.L. Mikhlin, L.E. Bykova, V.K. Mal'tsev, G.N. Bondarenko, Long-range chemical interaction in solid-state synthesis: the formation of a CuAu alloy in Au/β-Co(001)/Cu(001) epitaxial film structures, *JETP Lett.* 90 (2009) 111–115.
- [46] V.G. Myagkov, V.S. Zhigalov, B.A. Belyaev, L.E. Bykova, L.A. Solovyov, G.N. Bondarenko, Solid-state synthesis and magnetic properties of epitaxial FePd(001) films, *J. Magn. Magn. Mater.* 324 (2012) 1571–1574.
- [47] V.G. Myagkov, V.C. Zhigalov, L.E. Bykova, G.N. Bondarenko, Solid-state synthesis and phase transformations in Ni/Fe films: structural and magnetic studies, *J. Magn. Magn. Mater.* 305 (2006) 534–545.
- [48] V.G. Myagkov, V.C. Zhigalov, L.E. Bykova, G.V. Bondarenko, G.N. Bondarenko, Structural and magnetic features of the solid-state synthesis and martensitic transformations in Ni(0 0 1)/Mg(0 0 1) thin films, *J. Magn. Magn. Mater.* 310 (2007) 126–130.
- [49] V.G. Myagkov, O.A. Bayukov, L.E. Bykova, G.N. Bondarenko, The γ-Fe formation in epitaxial Cu(0 0 1)/Fe(0 0 1) thin films by the solid-state synthesis: structural and magnetic features, *J. Magn. Magn. Mater.* 321 (2009) 2260–2264.
- [50] V.G. Myagkov, L.E. Bykova, S.M. Zharkov, G.V. Bondarenko, Formation of NiAl shape memory alloy thin films by solid-state reaction, *Solid State Phenom.* 138 (2008) 377–384.
- [51] V.G. Myagkov, L.E. Bykova, L.A. Li, I.A. Turpanov, G.N. Bondarenko, Solid-phase reactions, self-propagating high-temperature synthesis, and martensitic transformations in thin films, *Dokl. Phys.* 47 (95) (2002) 95–98.
- [52] V.G. Myagkov, L.E. Bykova, G.N. Bondarenko, Solid-state synthesis and martensitic transformations in thin films, *Dokl. Phys.* 48 (2003) 30–33.
- [53] V.G. Myagkov, Yu.L. Mikhlin, L.E. Bykova, G.V. Bondarenko, G.N. Bondarenko, Long-range nature of chemical interaction in solid-phase reactions: formation of martensites phases of an Au-Cd Alloy in Cd/Fe/Au film systems, *Dokl. Phys. Chem.* 431 (2010) 52–56.
- [54] V.G. Myagkov, L.E. Bykova, G.N. Bondarenko, V.S. Zhigalov, Solid-phase synthesis of solid solutions in Cu/Ni(001) epitaxial nanofilms, *JETP Lett.* 88 (2008) 515–519. Cu/Ni.
- [55] V.S. Zhigalov, V.G. Myagkov, O.A. Bayukov, L.E. Bykova, G.N. Bondarenko, A.A. Matsynin, Phase transformations in Mn/Fe(001) films: structural and magnetic investigations, *JETP Lett.* 89 (2009) 621–625.
- [56] V.G. Myagkov, L.E. Bykova, G.N. Bondarenko, Superionic transition and self-propagating high-temperature synthesis of copper selenide in thin films, *Dokl. Phys.* 48 (5) (2003) 206–208.
- [57] S. Zhou, H. Schmidt, Mn-doped Ge and Si: a review of the experimental status, *Materials* 3 (2010) 5054–5082.
- [58] Y. Wang, F. Xiu, Y. Wang, X. Kou, A.P. Jacob, K.L. Wang, J. Zou, Mn-rich clusters in GeMn magnetic semiconductors: structural evolution and magnetic property, *J. Alloys Compd.* 508 (2010) 273–277.
- [59] T. Dietl, K. Sato, T. Fukushima, A. Bonanni, M. Jamet, A. Barski, S. Kuroda, M. Tanaka, Pham Nam Hai, H. Katayama-Yoshida, Spinodal nanodecomposition in semiconductors doped with transition metals, *Rev. Mod. Phys.* 87 (2015) 1311.
- [60] V.G. Myagkov, V.S. Zhigalov, A.A. Matsynin, L.E. Bykova, G.V. Bondarenko, G.N. Bondarenko, G.S. Patrin, D.A. Velikanov, Phase transformations in the Mn-Ge system and in Ge_xMn_{1-x} diluted semiconductors, *JETP Lett.* 96 (2012) 40–43.
- [61] V.G. Myagkov, V.S. Zhigalov, A.A. Matsynin, L.E. Bykova, Yu.L. Mikhlin, G.N. Bondarenko, G.S. Patrin, G.Yu. Yurkin, Formation of ferromagnetic germanides by solid-state reactions in 20Ge/80Mn films, *Thin Solid Films* 552 (2014) 86–91.
- [62] K.A. Avchaciov, W. Ren, F. Djurabekova, K. Nordlund, I. Sveklo, A. Maziewski, Modification of Pt/Co/Pt film properties by ion irradiation, *Phys. Rev. B* 92 (2015), 104109–1–104109–10.
- [63] J.X. Zhang, R.J. Zeches, Q. He, Y.-H. Chu, R. Ramesh, Nanoscale phase boundaries: a new twist to novel functionalities, *Nanoscale* 4 (2012) 6196–6204.
- [64] S. Yang, H. Bao, C. Zhou, Y. Wang, X. Ren, Y. Matsushita, Y. Katsuya, M. Tanaka, K. Kobayashi, X. Song, J. Gao, Large magnetostriction from morphotropic phase boundary in ferromagnets, *Phys. Rev. Lett.* 104 (2010), 197201–197201–4.
- [65] A. Murtaza, S. Yang, C. Zhou, M.T. Khan, A. Ghani, F. Tian, J. Wang, X. Song, M. Suchomel, Y. Ren, Structural and magnetic properties of morphotropic phase boundary involved Tb_{1-x}Gd_xFe₂ compounds, *J. Alloys Compd.* 680 (2016) 177–181.
- [66] D. Hunter, W. Osborn, K. Wang, N. Kazantseva, J. Hattrick-Simpers, R. Suchoski, R. Takahashi, M.L. Young, A. Mehta, L.A. Bendersky, S.E. Lofland, M. Wuttig, I. Takeuchi, Giant magnetostriction in annealed Co_{1-x}Fe_x thin-films, *Nat. Commun.* 2 (2011) 518.
- [67] R.M. Bozorth, *Ferromagnetism*, IEEE Press, New York, 1978.
- [68] T. Klemmer, D. Hoydick, H. Okumura, B. Zhang, W.A. Soffa, Magnetic hardening and coercivity mechanisms in L₁₀ ordered FePd ferromagnets, *Scr. Metall. Mater.* 33 (1995) 1793.
- [69] R.A. McCurrie, P. Gaunt, The magnetic properties of platinum cobalt near the equiatomic composition part I. the experimental data, *Philos. Mag.* 13 (1966) 567–577.
- [70] R.A. Ristau, K. Barmak, L.H. Lewis, K.R. Coffey, J.K. Howard, On the relationship of high coercivity and L₁₀ ordered phase in CoPt and FePt thin films, *J. Appl. Phys.* 86 (1999) 4527–4533.
- [71] M. Ohtake, S. Ouchi, F. Kirino, M. Futamoto, L₁₀ ordered phase formation in FePt, FePd, CoPt, and CoPd alloy thin films epitaxially grown on MgO(001) single-crystal substrates, *J. Appl. Phys.* 111 (2012), 07A708-1–07A708-3.
- [72] B.B. Maranville, A.L. Shapiro, F. Hellman, D.M. Schaad, E.T. Yu, Misfit-angle dependence of perpendicular magnetic anisotropy in thin epitaxial CoPt₃ films grown on vicinal MgO, *Appl. Phys. Lett.* 81 (2002) 517–519.